

# Finite Element Simulation of Al (2024) Adaptive Composites with Embedded Cu-Al-Ni SMA Particles

Kotresh M <sup>1</sup>, Dr. M. M. Benal <sup>2</sup>

<sup>1</sup> Research Scholar, Department of Mechanical Engineering, VTU RRC, Belgaum, Karnataka, India

<sup>2</sup> Professor & Head, Department of Mechanical Engineering, GEC, Kushalanagara, Karnataka, India

\*\*\*

**Abstract** - This study comprises finite element simulations of the shape memory effect due to the presence of SMA (shape memory alloy) particles in a composite. Finite element method (FEA) was performed using ANSYS Release 14, where the pre-strain was modeled by equivalent changes in the expansion coefficient of the SMA. Two case-studies were simulated and their predictions were compared: (a) the heating of a SMA composite without shape memory effect (SME), which causes deflection due to the difference in the expansion coefficients of matrix and particles and (b) the heating of a SMA composite with SME of particles, which includes the synergy of the shape memory effects of the matrix/particulate.

**Key Words:** FEA; adaptive composites; shape memory effect and ANSYS.

## 1. INTRODUCTION

Shape memory alloys (SMAs) have the ability to return to a predetermined shape when heated past the martensitic transformation, with the potential of reversible strains of several percent, generation of high recovery stresses and high power/weight ratios. The integration of fine SMA particles in particulate reinforced composites leads to so called adaptive composite materials. Such SMA composites can be used actively to control elastic modulus, internal stress state and natural vibration frequencies in the case of soft matrices and change shape in the case of soft matrices [1, 2]. It is well known that metal matrix composites (MMCs) exhibit a significant improvement in mechanical performance over unreinforced alloys in many commercial structural applications (Christman et al., 1989; Tvergaard, 1990; Derrien et al., 1999). In recent years they also have emerged as reasonable materials for military applications (Chin, 1999). These materials can have the highest performance in the desirable direction if continuous fibres are used. However, the utilization of continuous reinforcements is confined by high processing costs. Composites reinforced with discontinuous fibres or particles represent a good compromise between price and performance. There exist a variety of processing techniques for the production of aluminium based

composites with discontinuous ceramic reinforcements (Ibrahim et al. 1991; Harrigan, 1998). Parallel with the processing methods utilized to manufacture particulate reinforced MMCs (Lee and Sabramanian, 1992; Smagorinski et al., 1998; Tan and Zhang, 1998; Amigo et al., 2000), a number of analytical (Mori and Tanaka, 1972; Christensen and Lo, 1979; Pindera and Aboudi, 1988; Withers et al., 1989; Cristensen, 1990; Lee and Allen, 1993; Fotiuand Nemat-Nasser, 1996; Roatta et al., 1997) and numerical (Bao et al., 1991; Levy and Papazian, 1991; Llorca et al., 1991; Svobodnik et al. 1991; Zahl and McMeeking, 1991; Hom, 1992; Weissenbek and Rammerstorter, 1993; Weissenbek et al. 1994; Zahl and Schmauder, 1994a; Zahl et al., 1994; Li et al., 1995, 1999a,b; Dong and Schmander, 1996; Wilkinson et al., 1999; Bruzzi et al., 2001; Ji and Wany, in press) investigations of the mechanical properties of these composites have been developed. Numerical studies are usually based on the finite element technique and used for the optimisation of mechanical properties by changing of intrinsic parameters such as the inclusion volume fraction, aspect ratios and spatial arrangement of reinforcements. Typically these analyses assume a periodic distribution of reinforcements, so that a unit cell model is often employed. Though a particulate composite is generally considered as isotropic, nevertheless when applying the periodic microfield approach the simulated overall behaviour of the composite becomes anisotropic. Weissenbek et al. (1994) detailed different regular arrangements of inclusions and symmetry considerations. On the other hand, in real composites a microstructural anisotropy is frequently observed. Thus during the processing such as extrusion, ceramic particles tend to be aligned in stripes (Lee and Sabramanian, 1992; Poudens et al. 1995; Shyong and Derby, 1995; Tan and Zhang, 1998; Soppa et al., 1999). Taking into account the microstructural anisotropy, an anisotropy of mechanical properties should be expected. The purpose of the present paper is to investigate the mechanical behavior of composites reinforced with ceramic particles aligned in stripes. We systematically study composite strengthening as a function of degree of particle alignment and inclusion volume fraction, as composite strengthening has impact for failure in quasi-brittle systems.

## 2. FEA SIMULATION OF THE SHAPE MEMORY EFFECT OF AN SMA PARTICLES EMBEDDED IN AL (2024) MATRIX

The interaction between the embedded SMA and the host material is critical since most applications require transfer of load or strain from the particles to the host. In addition, the host material may have a pronounced effect on the local stress state and consequently the transformation behavior of the embedded SMA particles. This case-study is based on the experiments of Jonnalagadda et al [3] who measured the stress distribution during the SMA transformation by using the photo elastic technique. In the fabrication stage, they embedded a single Cu-Al-Ni particle of size 100 micron width 100 microns height and 100 microns thickness in an Al (2024) matrix which cured at room temperature. The particle was annealed at 600° C. Before it was embedded into the Al (2024), a uniform pre-strain was applied on it. The main problem seemed to be crack defect where, even with careful sample preparation, small crack of approximately 100 micron in length formed at the right and left side of the sample. The current study, first involved the construction of the 2-Dmodel of the experimental case, using ANSYS. It included two types of materials, the Al (2024) matrix and 20% SMA Cu-Al-Ni particles and the data for their properties are presented in Table 1. The experiment started at 10 °C at which the Cu-Al-Ni particles was in martensite state until 15 °C, then the phase transformation started from 16 °C (As) and the experiment stopped at 40 °C.

**Table 1** Material Properties of Al (2024) Matrix and Cu-Al-Ni SMA

Sl No	Properties	Al(2024)	Cu-Al-Ni SMA
1	Melting Point	502 - 638 °C	1000-1050 °C
2	Density ( $\rho$ )	2.78 gm/cc	7.12 gm/cc
3	Youngs Modulus (E)	73.1 GPa	80-85 GPa
4	Poisson's Ratio ( $\nu$ )	0.33	0.30
5	Thermal Conductivity (k)	121W/cc per °K	30-43W/cc per °C
6	CTE ( $\alpha$ )	24.7 $\mu\text{m}/\text{m}\cdot\text{°C}$	16-18 $\mu\text{m}/\text{m}\cdot\text{°C}$
7	Ultimate Tensile Strength	483 MPa	500-800 MPa
11	As	--	15 °C
12	Af	--	40 °C

where E is the Young's modulus,  $\nu$  is the Poisson's ratio,  $\alpha$  is the thermal expansion coefficient, K is the thermal conductivity,  $\rho$  is the density of the material,  $A_s$  is the Austenite start Temperature and  $A_f$  is the Austenite finish temperature. The FEA simulations consisted of a sequence of steady state thermal and structural analyses using ANSYS. In the former, it was assumed that the temperature

inside the particles was increasing at 1 °C/min. The solid, Quad 4 node 182 elements PLANE is selected for the thermal and structural analysis, respectively. The most difficult part of the structural analysis was to import into the ANSYS software the pre-strain that the particles had. Fig.1 presents a stress-strain graph, including the pre-straining stage.

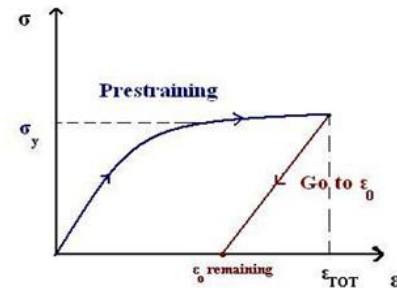


**Fig.1** Stress-strain graph for the pre-straining stage

From the graph in Fig. 1 and given that ANSYS was not able to incorporate initial strain conditions; an equation for the total strain was generated:

$$\epsilon_{TOT} = \epsilon_{ANSYS} + \epsilon_0 \quad (1)$$

The equation for the total stress is:

$$\sigma = E \epsilon_{ANSYS} + E \epsilon_0 \quad (2)$$

If it is assumed that the initial stress is equal to zero and equation 2 is interpolated for  $\epsilon_{ANSYS}$  between the two phases

(Martensite and Austenite), it yields

$$\epsilon_{ANSYS} = \left\{ \frac{[\sigma - E_{Aust} \epsilon_0 / E_{Aust} - \sigma / E_{Mart}] \times [T - A_s]}{A_s - A_f} \right\} \quad (3)$$

Equation 3 produces an equivalent expansion coefficient (positive as it really represents expansion), which is related to the shape memory effect between 15 and 40 °C and is given by

$$\alpha_x = \epsilon + 17 \times 10^{-6} \quad (4)$$

The results of the equivalent expansion coefficient for the Cu-Al-Ni Particles between the two phases are presented in Table 2. The fact that the expansion coefficient,  $\alpha$ , now incorporates the pre-straining effect, effectively makes  $\alpha$  anisotropic, depending on the pre-strain direction.

**Table 2.** Expansion coefficient of pre-strained Cu-Al-Ni SMA particles used in the ANSYS simulations.

Temp. °C	$\alpha_x$	$\alpha_y$
15	$17 \times 10^{-6}$	$17 \times 10^{-6}$
16	$4.56 \times 10^{-4}$	$17 \times 10^{-6}$
17	$17 \times 10^{-6}$	$17 \times 10^{-6}$
18	$17 \times 10^{-6}$	$17 \times 10^{-6}$
19	$17 \times 10^{-6}$	$17 \times 10^{-6}$

The change of the expansion coefficient  $\alpha_x$  stops at 16 °C, because the aim of the pre strain in the particles was achieved, so from 16 °C to 19 °C it is again  $17 \times 10^{-6}$  for all axes. First, a thermal FEA analysis was performed. There was a homogeneous initial temperature condition at 15 °C. The SMA particles between the Al (2024) matrix was heated up at a rate of 1 °C/min from a temperature of 15 °C to 19 °C.

### III. FEA SIMULATIONS Al (2024)/Cu-Al-Ni ADAPTIVE COMPOSITE WITHOUT PRE-STRAINING OF SMA PARTICLES:

The thermal analysis was followed by a steady state structural analysis. Fig.2 displays the stresses along the plane X, Y and XY direction. At this stage the composite has reached the maximum stresses at the regions of the matrix particulate interface and at both sides of the transverse crack tips. At this stage the particles are at 15 °C, the maximum  $\sigma_x$  value is at the interface of particle and matrix is 24.2MPa. Maximum  $\sigma_y$  values at the interface of particle and matrix is 24.3MPa and maximum value of shear stress is at 9.65MPa.

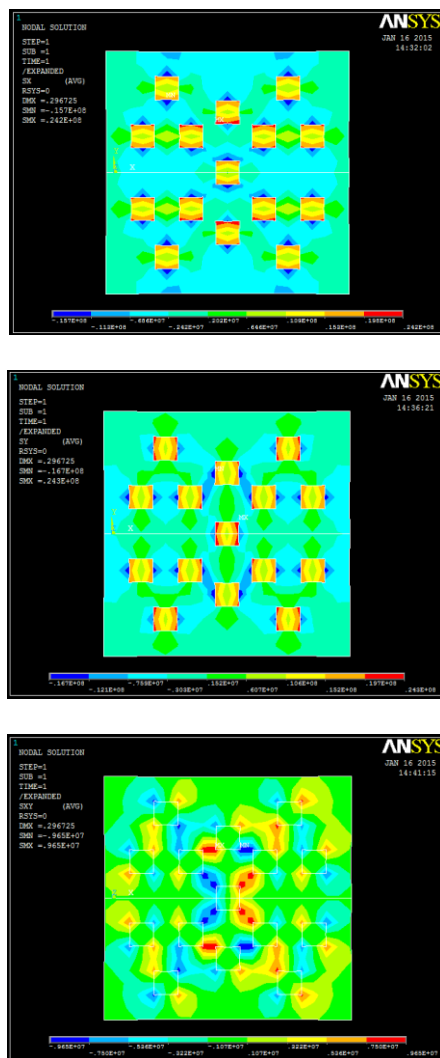
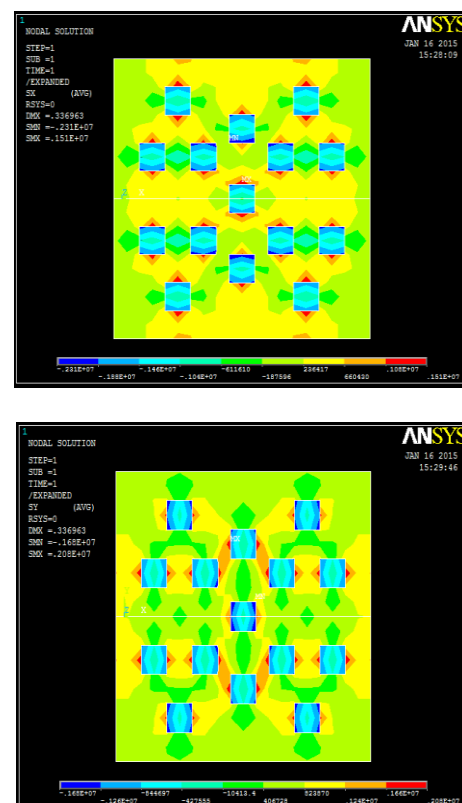


Fig 2 Stress values along X , Y and XY Planes without pre-straining(SME) the particulates

### IV. FEA SIMULATIONS Al (2024)/Cu-Al-Ni ADAPTIVE COMPOSITE WITH PRE-STRAINING OF SMA PARTICLES:

The thermal analysis and steady state structural analysis of composite with pre-straining of Cu-Al-Ni Particles are considered by varying the thermal coefficient of expansion. Fig.3 displays the stresses along the plane X, Y and XY direction. At this stage the composite has reached the maximum stresses at the regions of the matrix particulate interface and at both sides of the transverse crack tips. At this stage the particles are at 19 °C, the maximum  $\sigma_x$  value is at the interface of particle and matrix is 1.51MPa. Maximum  $\sigma_y$  value is at the interface of particle and matrix is 2.08MPa and maximum value of shear stress is at 0.904MPa. The graphical representation of varying stress values along x, y and xy plane subjected to both with and without shape memory effect as shown in fig.4,5& 6.



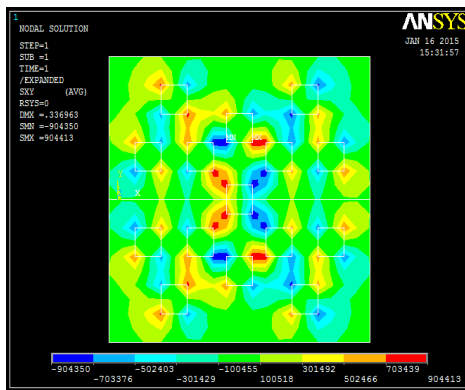


Fig 3. Stress values along X, Y and XY Planes with pre-straining (SME) the particulates

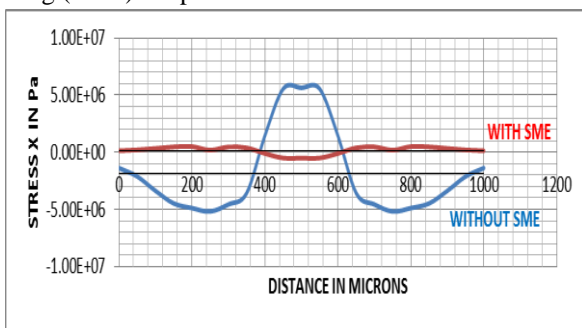


Fig.4 Variation of  $\sigma_x$  for composite with and without pre-strain (SME)

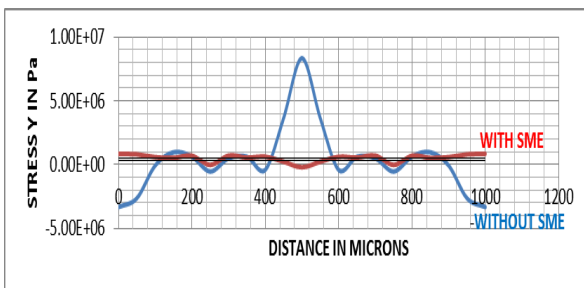


Fig.5 Variation of  $\sigma_y$  for composite with and without pre-strain (SME)

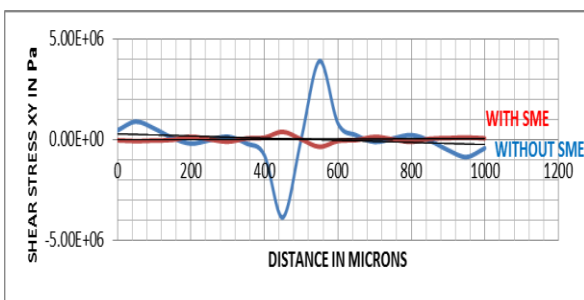


Fig.6 Variation of  $\tau_{xy}$  for composite with and without pre-strain (SME)

### V. CONCLUSIONS

The technique of employing a varying expansion coefficient to simulate the effects of pre-strain in SMA particles has been applied successfully in finite element analyses of the shape memory effect. The first case-study involved the shape memory effect of an SMA particles embedded in Al (2024) and demonstrated the problem of crack on either side of the composite, which demonstrates the stress values in X,Y and XY planes without pre-straining means shape memory effect. The second case-study involved Cu-Al-Ni SMA particles embedded in a Al (2024) composite in which the shape memory effect of the SMA particles-produces less oscillatory stress values at the region of the defect and at the interface, which means that composites embedded with SMA particles will reduce the effective performance of the defect.

### ACKNOWLEDGMENT

The author wish to thank the Executive Secretary, VGST, Bangalore, Karnataka, India for funding the project (Ref. no. VGST/K-FIST/2012-13/247, Dec 31, 2012) and also the Publishers.

### REFERENCES

- [1] Balta J.A., Parlinska M, Michaud V., Gotthardt R.,Manson J.-A.E Adaptive composites with embedded shape memory alloy wires, Proc. of the MRS Fall Meeting, Boston, 1999.
- [2] Friend C.M., Morgan N. The actuation response of model SMA hybrid laminates, J. de Physique, 1995, 5, C2 : 415-420
- [3] Jonnalagadda K.D., Sottos N.R., Qidwai M.A. and Lagoudas D.C. Transformation of embedded shape memory alloy ribbons, J. Intel. Mater. Sys. &Struct., 1998, 9(5): 379-390.
- [4] Behrens E. Thermal conductivities of composite materials, J. Comp. Mater., 1968, 2: 2-17.
- [5] Lindgren L E., “Finite Element Modeling and Simulation of Welding. Part 1: Increased Complexity”, Journal of Thermal Stresses, 24: 141-192, 2001
- [6] Smith M.C., Smith A.C., NeT Task Group 1 - Single bead on plate: “Review of phase 1 weld simulation round robin”, British Energy report E/REP/0089/GEN/05, 2005

- [7] Turski M., Edwards L., Pratihari S. and Zhang Y., "Residual Stress Measurement Using Neutron Diffraction and the Contour Method", 1<sup>st</sup> NET Workshop, Petten, The Netherlands, 2004
- [8] "Assessment of the Integrity of Structures Containing Defects", Procedure R6-Revision 4, British Energy, 2003
- [9] "Fitness-For-Service", API Recommended Practice 579, First Edition, American Petroleum Institute, Washington, D.C., 2000
- [10] Christman, T., Needleman, A., Suresh, S., 1989. An experimental and numerical study of deformation in metal-ceramic composites. *Acta Metall.* 37, 3029–3050.
- [11] Tvergaard, V., 1990. Analysis of tensile properties for whisker-reinforced metal-matrix composite. *Acta Metall. Mater.* 38, 185–194.
- [12] Derrien, K., Baptiste, D., Guedra-Degeorges, D., Foulquier, J., 1999. Multiscale modeling of the damaged plastic behavior and failure of AL/SiCp composites. *Int. J. Plasticity* 15, 667–685.
- [13] Ibrahim, I.A., Mohamed, F.A., Lavernia, E.J., 1991. Particulate reinforced metal matrix composites a review. *J. Mater. Sci.* 26, 1137–1156.
- [14] Harrigan Jr, W.C., 1998. Commercial processing of metal matrix composites. *Mater. Sci. Eng. A244*, 75–79.
- [15] Lee, J.C., Sabramanian, K.N., 1992. Effect of cold rolling on the tensile properties of (Al<sub>2</sub>O<sub>3</sub>)p/Al composites. *Mater. Sci. Eng. A159*, 43–50.
- [16] Smagorinski, M.E., Tsantrizos, P.G., Grenier, S., Cvasin, A., Brzezinski, T., Kim, G., 1998. The properties and microstructure of Al-based composites reinforced with ceramic particles. *Mater. Sci. Eng. A244*, 86–90.
- [17] Tan, M.J., Zhang, X., 1998. Powder metal matrix composites: selection and processing. *Mater. Sci. Eng. A244*, 80–85.
- [18] Amigo, V., Ortiz, J.L., Salvador, M.D., 2000. Microstructure and mechanical behavior of 6061Al reinforced with silicon nitride particles, processed by powder metallurgy. *Scripta Mater* 42, 383–388.
- [19] Mori, T., Tanaka, K., 1972. Average stress in matrix and average elastic energy of materials with misfitting inclusions. *Acta Metall.* 21, 571–574.
- [20] Christensen, R.M., Lo, K.H., 1979. Solutions for effective shear properties in three phase sphere and cylinder models. *J. Mech. Phys. Solids* 27, 315–330.
- [21] Lee, J.W., Allen, D.H., 1993. Axisymmetric micromechanics of elastic–perfectly plastic fibrous composites under uniaxial tension loading. *Int. J. Plasticity* 9, 437–460.
- [22] Fotiu, P.A., Nemat-Nasser, S., 1996. Overall properties of elastic–viscoplastic periodic composites. *Int. J. Plasticity* 12, 163–190.
- [23] Poudens, A., Bacroix, B., Bretheau, T., 1995. Influence of microstructures and particle concentrations on the development of extrusion textures in metal matrix composites. *Mater. Sci. Eng. A196*, 219–228.
- [24] Pindera, M.J., Aboudi, J., 1988. Micromechanical analysis of yielding of metal matrix composites. *Int. J. Plasticity* 4, 195–214.
- [25] Roatta, A., Turner, P.A., Bertinetti, M.A., Bolmaro, R.E., 1997. An iterative approach to mechanical properties of MMCs at the onset of plastic deformation. *Mater. Sci. Eng. A229*, 203–218.
- [26] Weissenbek, E., Rammerstorfer, F.G., 1993. Influence of the fiber arrangement on the mechanical and thermo-mechanical behaviour of short fiber reinforced MMCs. *Acta Metall. Mater.* 41, 2833–2843.
- [27] Weissenbek, E., Bo`hm, H.J., Rammerstorfer, F.G., 1994. Micromechanical investigations of arrangement effects in particle reinforced metal matrix composites. *Comp. Mater. Sci.* 3, 263–278.
- [28] Zahl, D.B., McMeeking, R.M., 1991. The influence of residual stress on the yielding of metal matrix composites. *Acta Metall. Mater.* 39, 1117–1122.
- [29] Zahl, D.B., Schmauder, S., McMeeking, R.M., 1994. Transverse strength of metal matrix composites reinforced with strongly bonded continuous fibers in regular arrangements. *Acta Metall. Mater.* 42, 2983–2997.

- [30] Levy, A., Papazian, J.M., 1991. Elastoplastic finite element analysis of short-fiber—reinforced SiC/Al composites: effects of thermal treatment. *Acta Metall. Mater.* 39, 2255–2266.